TABLE 1. (*Continued*)

Primers	Stage-polarity	Nucleotide sequence (5′–3′)
Primer set 18	1st sense	GGGTGGAATGAATAACATGTCT
	2nd sense	CAACCCGGTACTGGGCATAA
	1st antisense	ATGCGCCCTCGGCCTATTTTG
	2nd antisense	ATGRGTATTGGTRCCGTCCTG
Primer set 19	1st sense	TTGGCGTGACCAGGCCCAGCG
	2nd sense	GCCATGTATRCARAGCATAACAAG
	1st antisense	GTAGACCTRCCACAGCTGGG
	2nd antisense	GCCTCCTCCTCMGCCACCCC
Primer set 20	1st sense	ACCACCACCCCGACGTCCGT
	2nd sense	TGTCAGCAAGGTTRAACAGGG
	1st antisense	ATAACYTCGACKGATGTTCG
	2nd antisense	GCTATCCCGCGGCCGATCTC
Primer set 21	1st sense	CGCAACCTYACCCCYGGTAA
	2nd sense	GGACTGGTCATACTCGGCAGC
	1st antisense	GTCTCCCGTTAYTCCAGCAC
	2nd antisense	AGAGARAGCCAAAGCACATC
Primer set 22	1st sense	ACAGAATTGATTTCGTCGGC
	2nd sense	TAATTATAAGGGTACCCGG
	1st antisense	CTGTAGAGAATGCTCAGCAGG
	2nd antisense	CGRAGCGGCAGGACAAAGAA
Primer set 23	1st sense	TCYGACTCTGTGACCTTGGT
	2nd sense	CAAGCAAATAAACTATAACTCCCG
	1st antisense	ACCGGCGCGCAGGCCGTTG
	2nd antisense	GTTTTACCCACCTTCATCTTAAGG

Bangladesh (MITR 1–17) (Fig. 2). The HEV sequences of the 15 isolates from Rajshahi were also similar to HEV isolates from India, Burma, China, and Nepal (Fig. 2).

Comparison of the Almost Complete nt Sequences of Two HEV Isolates From Bangladesh and Other Reported HEV Isolates

The almost complete genome sequences of the two HEV isolates with high levels of HEV RNA (E11-Ban 10 and E13-Ban10) were evaluated (Fig. 3). These patients who were the sources of these isolates presented to the physician on February 10, 2010 (E11-Ban10) and February 11, 2010 (E13-Ban10) and they lived in close proximity. The nucleotide sequences of both HEV isolates contained 7,186 nt, which comprised the 5′UTR (nt 1–5), ORF1 (nt 6–5,087 for 1,693 amino acids [aa]), ORF2 (nt 5,125–7,107 for 660 aa), ORF3 (nt 5,084–5,455, for 122 aa), 3′UTR (nt 7,108–7,172), and poly-A tail (nt 7,173–7,186). The almost complete genome sequences had 14 mismatched nts in the two Bangladeshi isolates, E11-Ban10 and E13-Ban10. These two Bangladeshi isolates shared 92.9–94.5% sequence homology with HEV genotype 1a isolates from India (DQ459342,

TABLE II. Profiles of the Patients [A]

Parameters	Data
Age (years)	29.3 ± 10.1 (range: 3–60 years)
Sex	
Male	177
Female	23
Occupation	
Student	94
Service holder	33
Farmer	24
Businessman	25
House wives	24
Residence	
Urban	121
Rural	79

TABLE III. Clinical and Laboratory Profiles of the Patients

Parameters	Numbers of patients
[A] Clinical profiles of the patients	
Anorexia	200
Nausea	200
Vomiting	199
Abdominal pain	198
Pruritis	32
Loose motion	88
Weight loss	30

Parameters	Mean and standard deviation
[B] Laboratory profiles of the patients	
Serum bilirubin (mg/dl)	5.9 ± 3.0 (range: 1.6–20.2 mg/dl)
Serum alanine aminotransferase (IU/L)	733 ± 533 (range: 41–2,971 IU/L)
IgM type antibody to	
Hepatitis A virus	0
Hepatitis B virus	0
Hepatitis C virus	0
Hepatitis E virus	200
Hepatitis B surface antigen	20
Anti-hepatitis C virus	14

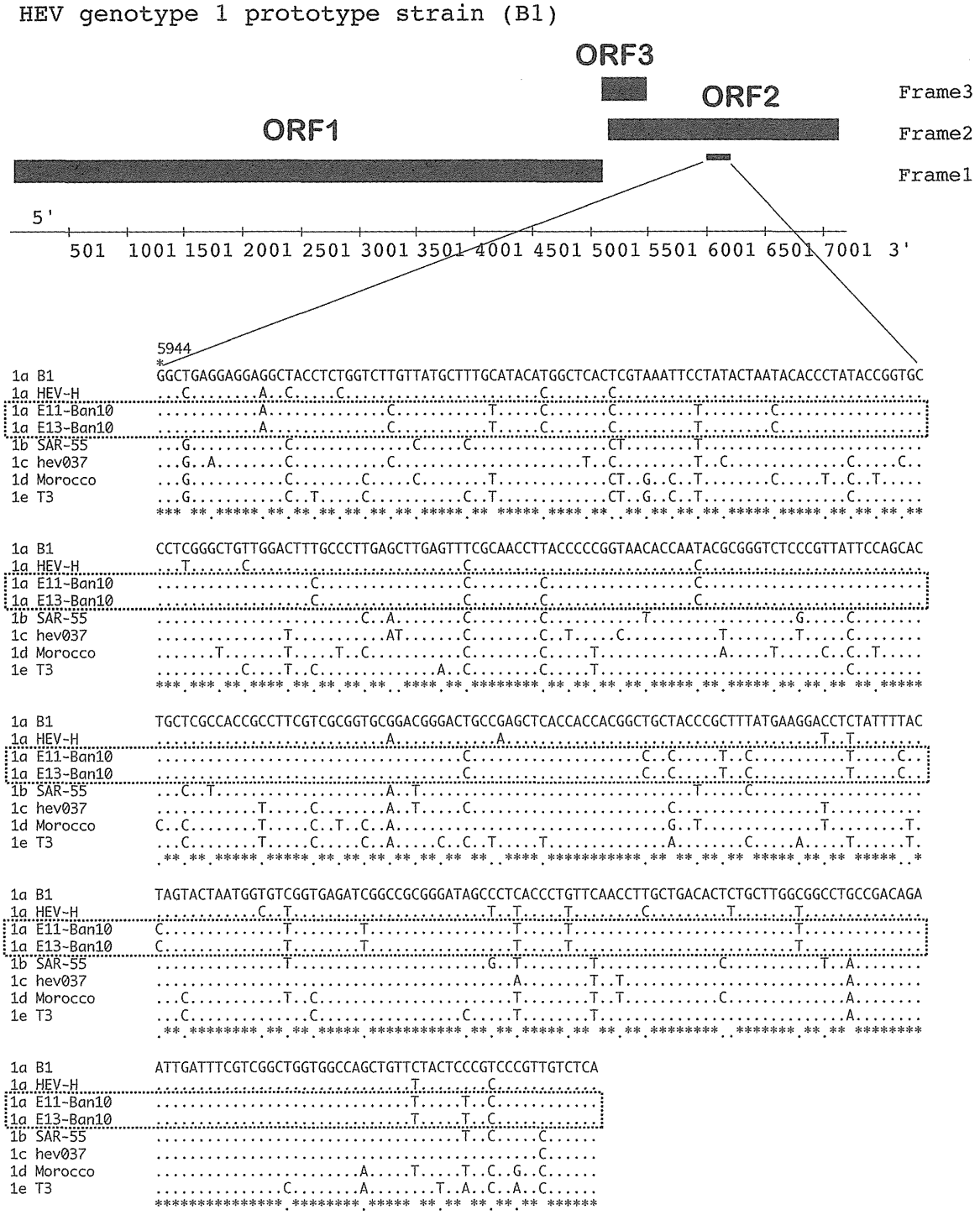

Fig. 1. Genetic map of HEV genotype 1, showing the region of nucleotide sequence determined for phylogenetic analysis in this study.

X99441, AF076239, and FJ457024). They also shared 91.9–92.3% sequence homology with HEV genotype 1b isolates from Pakistan (AF444002, AF444003, and M80581) and China (L25547, L25595, M94177, L08816, D11092, and D11093). The Bangladeshi HEV isolates shared 91.9% sequence homology with HEV genotype 1c isolates (X98292, India), 88.2–88.3% sequence homology with HEV genotype 1d (AY230202, Morocco), 88.7% sequence homology with HEV genotype 1e (AY204877, Chad), 75.8% sequence homology with genotype 2 (M74506, Mexico), 73.9% sequence homology with genotype 3 (AF060669, USA), and 74.3% sequence homology with HEV genotype 4 (AY723745, India). An outgroup HEV genotype that

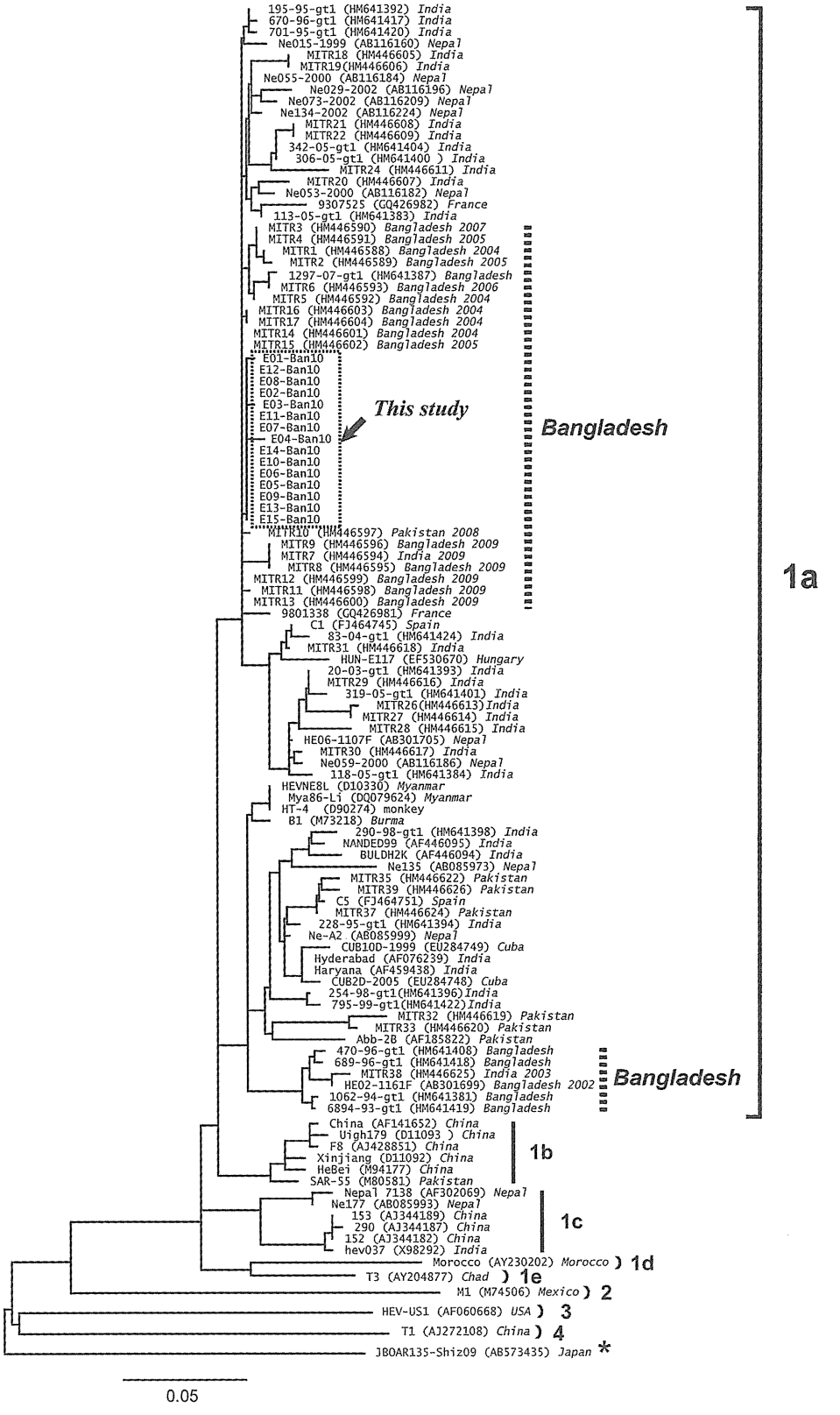

Fig. 2. Phylogenetic tree constructed using the neighbor-joining method based on the partial nucleotide sequence of the ORF2 region (266 nt) from 115 HEV isolates, including 15 HEV isolates in this study. The 15 HEV isolates obtained in the present study are indicated by the dotted square (an arrowhead indicates ***This study***). The reported isolates of HEV genotypes **1a**, **1b**, **1c**, **1d**, **1e**, **2**, **3**, and **4**, as well as an outgroup (shown by an asterisk) included for comparison, and their GenBank accession numbers are shown in parentheses.

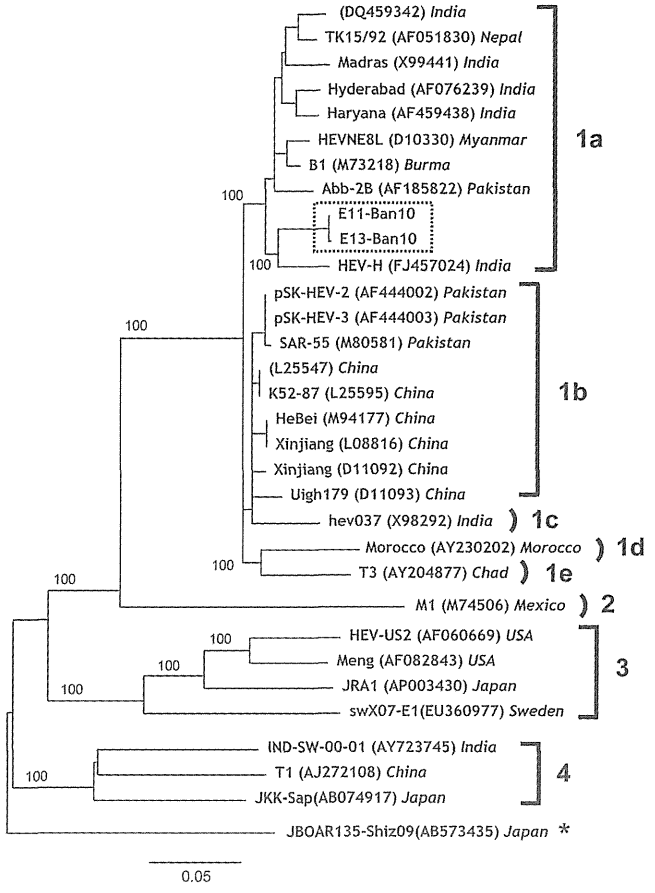

Fig. 3. Phylogenetic tree constructed using the neighbor-joining method based on the almost complete HEV sequences of two Bangladeshi HEV isolates (E11-Ban10 and E13-Ban10) (shown by the dotted square). The reported full genome sequences of HEV genotypes **1a**, **1b**, **1c**, **1d**, **1e**, **2**, **3**, and **4**, as well as an outgroup (shown by an asterisk) included for comparison, and their GenBank accession numbers are shown in parentheses.

shared 73.7% sequence homology is shown at the end of Figure 3 (AB573435, Japan), which was isolated from a wild boar [Takahashi et al., 2010].

DISCUSSION

Hepatitis caused by HEV of Bangladeshi origin was first reported among patients from The Netherlands who developed acute hepatitis E after traveling to Bangladesh [Zaaijer et al., 1993]. Greater attention was focused on HEV in Bangladesh when United Nations peace-keepers from Bangladesh exhibited acute hepatitis E during their assignment in Haiti, while patients from Japan, Spain, and Italy also developed acute hepatitis E after traveling to Bangladesh [Drabick et al., 1997; Sanayama et al., 2008; Fogeda et al., 2009; La Rosa et al., 2011; Romanò et al., 2011]. However, the epidemiology of HEV-induced acute hepatitis E and the genomic features of HEV in Bangladesh have not been investigated adequately.

The present study provides some important insights into the epidemiology of acute hepatitis E in Bangladesh. It is not clear why patients with acute hepatitis E, rather than acute hepatitis A, visited physicians at Rajshahi during January and February in 2010 but there may be two main reasons. First, only patients with severe acute hepatitis visited physicians so other patients with acute hepatitis and comparatively mild symptoms may not have visited physicians. The second cause may be related to the timing of the outbreak. In general, waterborne acute icteric hepatitis outbreaks caused by HEV and HAV occur during August or September in Asian developing countries at the end of the monsoon season, or during/after flooding [Hlady et al., 1990; Naik et al., 1992; Purcell and Emerson, 2000]. However, the present episode of acute hepatitis E was detected during the winter (January and February 2010) and there were no other acute hepatitis epidemics in Bangladesh at that time. Thus, the non-seasonal outbreak of acute hepatitis E that started in January 2010 and ended in February 2010 (winter season) in Rajshahi may have been due to the contamination of a common source by HEV.

The genomic analysis showed that HEV isolates from 15 patients with acute hepatitis E belonged to HEV genotype 1a, which formed a single cluster in the phylogenetic tree (Fig. 2). The almost complete nt sequences of the HEV genomes recovered from two patients had 14 mismatched nts (E11-Ban 10 and E13-Ban10). Thus, it is possible that HEV strains with high pathogenic potential are endemic in and around the Rajshahi area. They may have experienced natural mutation at a rate of 1.40×10^{-3} base substitutions per site per year, as previously described [Takahashi et al., 2004]. This may explain the 14 mismatched nts between the two HEV isolates. The two Bangladeshi HEV isolates also shared more than 90% sequence homology with a HEV genotype 1a isolate from India, HEV genotype 1b isolates from Pakistan, China, and India, and a HEV genotype 1c isolate from India. HEV genotypes 1a is highly prevalent in India [Kumar et al., 2011] and Pakistan [Iqbal et al., 2011], two close neighbors of Bangladesh.

In addition to the information provided in this study of HEV in Bangladesh, this study also detected a high prevalence of HBV and HCV in patients with acute hepatitis E in this cohort (Table III [B]). This indicates the challenging issue of coinfection with HEV, HBV, and HCV in Rajshahi, Bangladesh.

In conclusion, this study showed that a sudden outbreak of acute icteric hepatitis due to HEV occurred in the winter in Bangladesh, but not after flooding. The HEV genotype was assessed in this study. This appears to be the first study to evaluate the almost complete gene sequences of HEV from Bangladeshi patients. This study was conducted in Bangladesh so it may help policy-makers in Bangladesh to recognize the extent of the HEV-related public health problem.

REFERENCES

Al-Mahtab M, Rahman S, Khan M, Karim F. 2009. HEV infection as an aetiologic factor for acute hepatitis: Experience from a tertiary hospital in Bangladesh. J Health Popul Nutr 27:14–19.

Balayan MS, Andjaparidze AG, Savinskaya SS, Ketiladze ES, Braginsky DM, Savinov AP, Poleschuk VF. 1983. Evidence for a virus in non-A, non-B hepatitis transmitted via the fecal-oral route. Intervirology 20:23–31.

Drabick JJ, Gambel JM, Gouvea VS, Caudill JD, Sun W, Hoke CH, Jr., Innis BL. 1997. A cluster of acute hepatitis E infection in United Nations Bangladeshi peacekeepers in Haiti. Am J Trop Med Hyg 57:449–454.

Fogeda M, Avellón A, Cilla CG, Echevarría JM. 2009. Imported and autochthonous hepatitis E virus strains in Spain. J Med Virol 81:1743–1749.

Hlady WG, Islam MN, Wahab MA, Johnson SD, Waiz A, Krawczynski KZ. 1990. Enterically transmitted non-A, non-B hepatitis associated with an outbreak in Dhaka: Epidemiology and public health implications. Trop Doct 20:15–17.

Iqbal T, Idrees M, Ali L, Hussain A, Ali M, Butt S, Yousaf MZ, Sabar MF. 2011. Isolation and characterization of two new hepatitis E virus genotype 1 strains from two mini-outbreaks in Lahore, Pakistan. Virol J 8:94.

Kumar S, Pujhari SK, Chawla YK, Chakraborti A, Ratho RK. 2011. Molecular detection and sequence analysis of hepatitis E virus in patients with viral hepatitis from North India. Diagn Microbiol Infect Dis 71:110–117.

La Rosa G, Muscillo M, Vennarucci VS, Garbuglia AR, La Scala P, Capobianchi MR. 2011. Hepatitis E virus in Italy: Molecular analysis of travel-related and autochthonous cases. J Gen Virol 92:1617–1626.

Labrique AB, Zaman K, Hossain Z, Saha P, Yunus M, Hossain A, Ticehurst J, Nelson KE. 2009. Population seroprevalence of hepatitis E virus antibodies in rural Bangladesh. Am J Trop Med Hyg 81:875–881.

Naik SR, Aggarwal R, Salunke PN, Mehrotra NN. 1992. A large waterborne viral hepatitis E epidemic in Kanpur, India. Bull World Health Organ 70:597–604.

Purcell RH, Emerson SU. 2000. Hepatitis E virus infection [letter]. Lancet 355:578.

Ray R, Aggarwal R, Salunke PN, Mehrotra NN, Talwar GP, Naik SR. 1991. Hepatitis E virus genome in stools of hepatitis patients during large epidemic in north India. Lancet 338:783–784.

Romanò L, Paladini S, Tagliacarne C, Canuti M, Bianchi S, Zanetti AR. 2011. Hepatitis E in Italy: A long-term prospective study. J Hepatol 54:34–40.

Sanayama Y, Ishiwada N, Fukasawa C, Kanazawa M, Tamano Y, Yano K, Kohno Y. 2008. A pediatric patient with acute hepatitis E in Japan. J Infect Chemother 14:374–376.

Sheikh A, Sugitani M, Kinukawa N, Moriyama M, Arakawa Y, Komiyama K, Li TC, Takeda N, Ishaque SM, Hasan M, Suzuki K. 2002. Hepatitis e virus infection in fulminant hepatitis patients and an apparently healthy population in Bangladesh. Am J Trop Med Hyg 66:721–724.

Shrestha SM, Sherestah S, Tusda F, Nishizawa T, Gotanda Y, Takeda N, Okamoto H. 2003. Molecular investigation of hepatitis E virus infection in patients with acute hepatitis in Kathmandu, Nepal. J Med Virol 69:207–214.

Takahashi K, Toyota J, Karino Y, Kang J-H, Abe N, Mishiro S. 2004. Estimation of the mutants rate of hepatitis E virus based on a set of closely related 7.5-year apart isolates from Sapporo, Japan. Hepatol Res 29:212–215.

Takahashi K, Okamoto H, Abe N, Kawakami M, Matsuda H, Mochida S, Sakugawa H, Suginoshita Y, Watanabe S, Yamamoto K, Miyakawa Y, Mishiro S. 2009. Virulent strain of hepatitis E virus genotype 3, Japan. Emerg Infect Dis 15:704–709.

Takahashi K, Terada S, Kokuryu H, Arai M, Mishiro S. 2010. A wild bore-derived hepatitis E virus isolate presumably representing so far unidentified 'genotype 5'. Kanzo (abstract in English) 51:536–538.

Ticehurst J, Popkin TJ, Bryan JP, Innis BL, Duncan JF, Ahmed A, Iqbal M, Malik I, Kapikian AZ, Legters LJ. 1992. Association of hepatitis E virus with an outbreak of hepatitis in Pakistan: Serologic responses and pattern of virus excretion. J Med Virol 36:84–92.

Zaaijer HL, Kok M, Lelie PN, Timmerman RJ, Chau K, van der Pal HJ. 1993. Hepatitis E in The Netherlands: Imported and endemic. Lancet 341:826.

Journal of Virology

The Hepatitis E Virus Capsid C-Terminal Region Is Essential for the Viral Life Cycle: Implication for Viral Genome Encapsidation and Particle Stabilization

Tomoyuki Shiota, Tian-Cheng Li, Sayaka Yoshizaki, Takanobu Kato, Takaji Wakita and Koji Ishii
***J. Virol.* 2013, 87(10):6031. DOI: 10.1128/JVI.00444-13.**
Published Ahead of Print 6 March 2013.

JVI
Journals.ASM.org

The Hepatitis E Virus Capsid C-Terminal Region Is Essential for the Viral Life Cycle: Implication for Viral Genome Encapsidation and Particle Stabilization

Tomoyuki Shiota, Tian-Cheng Li, Sayaka Yoshizaki, Takanobu Kato, Takaji Wakita, Koji Ishii

Department of Virology II, National Institute of Infectious Diseases, Gakuen, Musashi-murayama, Tokyo, Japan

Although the C-terminal 52 amino acids (C52aa) of hepatitis E virus (HEV) capsid are not essential for morphology, the C52aa-encoding region is required for replication. Transfection of a C52aa knockdown mutant showed transient growth, and the earliest population included a majority of noninfectious (possibly empty) particles and a minority of infectious particles with C-terminal capsid degradation. Finally, the complete revertant was generated reproducibly. C52aa is essential for the viral life cycle, promoting accurate encapsidation and stabilizing encapsidated particles.

Hepatitis E virus (HEV) is responsible for acute and enterically transmitted hepatitis in the developing world (1). Before the establishment of high-efficiency HEV cell culture systems (2), *in vitro* generation of HEV virus-like particles (HEV-VLPs) in insect cells and *in vivo* propagation in nonhuman primates were the most useful models for the study of HEV. Genetic deletions or cellular processing resulting in the loss of the N-terminal 111 or 13 amino acids (aa) or of the C-terminal 52 aa (C52aa) yielded capsid protein capable of directing the formation of the HEV small (S) or large (L) VLPs (3–5). Particle formation was required for C52aa abbreviation, limiting the structural analysis of the resulting particles (3, 4, 6–10). However, the contribution of the C52aa-encoding sequence was confirmed by both *in vivo* (attenuated infectivity of the point mutant virus in nonhuman primates) and *in vitro* (reduced RNA synthesis by RNA-dependent RNA polymerase [RdRp]) assays (11–14). Furthermore, the highly conserved nature of the C52aa sequence implies that the C52aa domain itself is functionally important. In this study, we characterized the role of the C52aa domain in the HEV life cycle by using infectious clones.

We constructed infectious clones by using the infectious virus G3-HEV83-2-27, employing a procedure described previously (20). Using a synthetic cDNA as the template, we amplified 12 fragments covering the entire G3-HEV83-2-27 genome by PCR with the primers listed in Table 1. These fragments were ligated stepwise and were inserted into the EcoRI-HindIII site of pUC19, yielding a wild-type clone that we designated WT. Site-directed mutagenesis of WT was used to generate clones that were mutated to encode capsid protein lacking the C52aa domain, either by introduction of an amber stop codon, UAA (a knockdown mutant designated Amut), or via deletion of the corresponding segment of the open reading frame 2 (ORF2) sequence (a knockout mutant designated Dmut). We performed experiments on three separate scales (normal, large, and huge, as described below) in order to estimate virus progeny productivity, to clarify the growth kinetics, and to analyze the process of encapsidation in the absence of revertants.

Normal scale. To estimate the virus progeny productivity of HEV without C52aa, transfection with Amut and Dmut was performed in comparison to transfection with WT. A 50-μg quantity of RNA from each infectious clone was electroporated into 1×10^7 cells of PLC/PRF/5. Analysis by enzyme-linked immunosorbent assay (ELISA) (using an anti-G3-HEV-VLP rabbit polyclonal antibody [5]) suggested that transient growth was observed with Amut, in contrast to continuous growth with WT (Fig. 1A) and no growth with Dmut (data not shown). The productivity (expressed as the genome copy number) of Amut, measured by real-time reverse transcription-PCR (RT-PCR) of RNA with a set of specific primers (Table 1), was estimated as approximately 40-fold lower than that of WT (Fig. 1B and 1C; note the differences in scale). However, subsequent analysis demonstrated that the Amut-derived HEV actually harbored synonymous and nonsynonymous reversion mutations, suggesting that the actual productivity (of intact Amut) was much lower than that suggested by real-time RT-PCR. To assess the progeny, sucrose density gradient analysis (SDGA) (with a gradient from 10 to 60% [wt/vol] sucrose) was performed. Subsequently, the collected fractions were separated by sodium dodecyl sulfate-polyacrylamide gel electrophoresis (SDS-PAGE), and Western blot analysis (WB) was performed with the polyclonal antibody noted above (5). Chemiluminescence was recorded using an LAS-3000 luminescent image analyzer (Fujifilm, Tokyo, Japan). In the series of fractions obtained from progeny derived from infection with WT, the presence of antigen was confirmed only in fraction 8 (F8) in Fig. 1C by WB (data not shown). The 72-kDa size of the prominent band was in agreement with the size of the capsid protein predicted for the WT clone. Quantification of the HEV RNA genome copy number showed a trailing peak for the progeny derived from infection with Amut (Fig. 1B, F8 and F9) and a single peak for the progeny derived from infection with WT (Fig. 1C, F8). These peaks corresponded to similar specific densities. Sequence analysis showed that while the progeny from infection with WT carried the original sequence, the progeny from infection with Amut did not contain the expected UAA (amber codon) at this position. Instead, the trailing peak of this Amut-derived sample corresponded to two

Received 12 February 2013 Accepted 22 February 2013
Published ahead of print 6 March 2013
Address correspondence to Koji Ishii, kishii@nih.go.jp.

doi:10.1128/JVI.00444-13

TABLE 1 Primers used for the construction of an HEV infectious cDNA clone, the C52aa deletion mutant, and the amber mutant and for the quantification and sequencing of HEV RNA by real-time RT-PCR

Name	Polarity[a]	Sequence (5′–3′)	Position in genome (nt)[b]	Amplicon (amplified region in genome [nt])[b]
ET7G2-F	+	GAATTCAATACGACTCACTATAGGCAGACCACGTATGTGGTCGAT[c]	2–23	Fragment 1-1 (2–155)
155R-EV	−	AGTCTGCACGCGAGATAAAAACGGCCGGAC	126–155	
126F-EV	+	GTCCGGCCGTTTTTATCTCGCGTGCAGACT	126–155	Fragment 1-2 (126–1370)
1370R-EV	−	CACCCTGGGATCCAGATGGAAGCCCGCAG	1342–1370	
1363F-EV	+	TCTGCGGGCTTCCATCTGGATCCCAGGGTG	1341–1370	Fragment 2-1 (1341–1794)
1816R-EV	−	ACTGCTCAGGGCCGTTCGCCTCAAGATGAG	1765–1794	
1787F-EV	+	CTCATCTTGAGGCGAACGGCCCTGAGCAGT	1765–1794	Fragment 2-2 (1765–2934)
2956R-EV	−	CGGCACAGGCACGGCCAACCTCTGTGGCAG	2905–2934	
2857F-EV	+	CCGATGCAGCCGGCACTCACAATAACGGAG	2835–2864	Fragment 3-1 (2835–3194)
3216R-EV	−	AGCCCGCTGCATATGTAATAGCAGCAAGTG	3165–3194	
3187F-EV	+	CACTTGCTGCTATTACATATGCAGCGGGCT	3165–3194	Fragment 3-2 (3165–3925)
3947R-EV	−	TCCGTAAGCTCAAAAACCAACACACTATCG	3896–3925	
3918F-EV	+	CGATAGTGTGTTGGTTTTTGAGCTTACGGA	3896–3925	Fragment 3-3 (3896–4598)
4620R-EV	−	CTTCCAAAACCCCTTAAGGGATTCCTTAGG	4569–4598	
4591F-EV	+	CCTAAGGAATCCCTTAAGGGGTTTTGGAAG	4569–4598	Fragment 4-1 (4569–5406)
5428R-EV	−	CTGTCGAGGGCGAGCTCCAGCCCCGGATTG	5377–5406	
5399F-EV	+	CAATCCGGGGCTGGAGCTCGCCCTCGACAG	5377–5406	Fragment 4-2 (5377–5851)
5873R-EV	−	TGGAGTTCATGTCAACAGAAGTAGGGGTAG	5822–5851	
5844F-EV	+	CTACCCCTACTTCTGTTGACATGAACTCCA	5822–5851	Fragment 4-3 (5822–6185)
6207R-EV	−	GTTCCATCGGCACCGCGGCGCAGCCGATG	6157–6185	
6179F-EV	+	CATCGGCTGCGCCGCGGTGCCGATGGAAC	6157–6185	Fragment 5-1 (6157–7101)
7101R-EV	−	AGTAGACTGGAAGGCGCAACCCTGC	7077–7101	
6981F-EV	+	CTGCGGTCGGTGTGTTAGCTCCACACTCGG	6959–6988	Fragment 5-2 (6959–7266)
SmartIIA-Hind	−	GCTCGAGCGGCCGCCAGTGTGATGGATATCTGCAGAATTCG GCTTAAGCAGTGGTATCAACGCAGAAAGCTTTTTTTTT TTTTTTTTTTTTTTTTTT[d]	7238–7266	
D81-F	+	ATGTGCCCTAGGGCTGTTCTGTTG	5173–5196	D81F/ORF2-52aa-Pac-R (5173–6995)
ORF2-52aa-Pac-R	−	AATTAATTAATTAAGCAAGGGCCGAGTGTGGAG[e]	6977–6995	
ORF2-52aa-del-F	+	TCCACACTCGGCCCTTGCTTAACTTGAGGATACTATTGACTAT[f]	6978–7020	
ORF2-52aa-del-R	−	ATAGTCAATAGTATCCTCAAGTTAAGCAAGGGCCGAGTGTGGA[f]	6978–7020	D81-F/ORF2-52aa-del-R (5173–7020)
7224R	−	AGGGAGCGCGAAAAGCAGAAAAGAAAAAT	7196–7224	ORF2-52aa-del-F/7224R (6978–7224)
HEV-G3-ANYF	+	ACCCCGGCAGTTGGTTTT	179–196	HEV-G3-ANYF/ANYR (179–234)
HEV-G3-ANYR	−	CCCGCTGGATAGGATGATTCC	212–234	
HEV-G3-ANYM1	+	FAM-CGCCCTGAGGTACTT-BHQ-1[g]	198–212	
83-2-6564F	+	GCTTCGTGCTAATGATGTTCTGTG	6564–6587	83-2-6564F/3′-terminal end (6564–7266)
83-2-6940F	+	CACCCAGGCTAGTGGTGTAGGTAGA	6940–6964	83-2-6940F/3′-terminal end (6940–7266)
ORF2-R-pacI	−	GAGAATTAAGACTCCCGGGTTTTAC	7136–7160	83-2-6564F/ORF2-R-pacI (6564–7160)

[a] Polarity of the primer on the HEV genome. +, forward; −, reverse.
[b] In G3-HEV83-2-27 (GenBank accession no. AB740232).
[c] The underlined sequence contains the T7 promoter.
[d] The underlined sequence contains a SmartIIA-specific sequence and a HindIII-digestible sequence.
[e] The underlined sequence contains a PacI-digestible sequence.
[f] The mutated nucleotides are underlined.
[g] The fluorophore 6-carboxyfluorescein (FAM) is attached to the 5′ end of the probe, and a quencher, Black Hole Quencher-1 (BHQ-1), is attached to the 3′ end.

distinct peaks (F8 and F9) harboring the GUU (Val-encoding) and GAC (Asp-encoding) codons, respectively. These changed RNA sequences were predicted to encode full-length revertant capsid proteins.

Large scale. To clarify the precise growth kinetics of Amut, a larger-scale transfection of Amut RNA was performed. Specifically, the large-scale transfection was performed on a scale approximately 30-fold larger than that described above, and culture supernatants were collected periodically. This procedure permitted a time course of quantification by ELISA analysis and showed that the peak of antigen accumulation occurred 25 days posttransfection, while the number of viral genomes progressively declined during the 2 months of the study (except for small recoveries in copy number on day 25 and at the end of the study) (Fig. 2A). These data suggested the production of a low level of infectious particles from Amut transfection. However, the nonreverted Amut antigens could not be distinguished by WB in the normal- and large-scale experiments, suggesting that the Amut products were unstable, of low infectivity, and/or produced in small amounts. To confirm the nature of the Amut product, pooled supernatants were subjected to partial purification and SDGA. WB of the resulting fractions detected a 72-kDa band in F7 (specific density, 1.15 g/ml) (Fig. 2B). Quantification of the HEV RNA genome in the fractions detected a single peak, primarily in F7 (Fig. 2C). Determination of the F7 sequence revealed that the codon expected to be an amber codon was instead GUC (complete reversion). Additionally, infection assays demonstrated that F7 readily infected cells (Fig. 2D). Based on our subsequent experiments, we suspect that the end product of the large-scale experiment likely corresponded to a revertant to WT.

Huge scale. To clarify the apparent reversion of Amut, transfection was performed at an even larger scale (10-fold increased over the large scale); culture supernatants were collected periodically, and viral sequences from these samples were determined. The results clearly showed a population shift from the originating amber codon of Amut to the complete revertant (GUC) via an intermediate mutant (GAC) (Table 2). Reversion mutants were

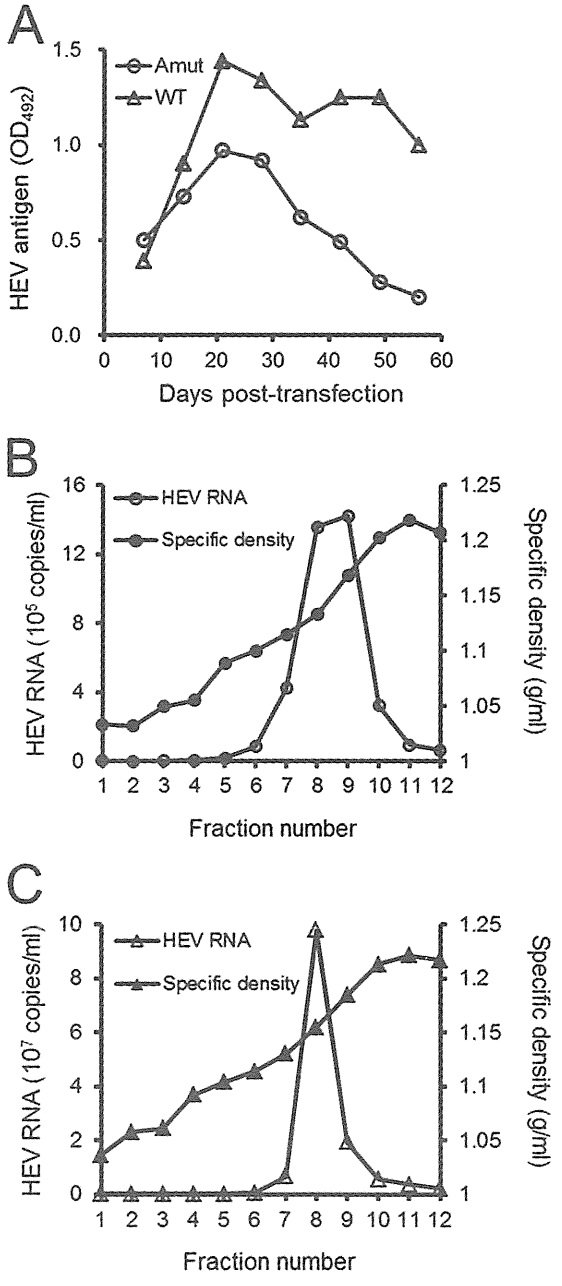

FIG 1 Initial characterization of Amut and WT HEV. (A) Time course of antigen production following transfection with Amut or WT HEV. HEV antigen levels were measured by ELISA using an anti-G3-HEV-VLP rabbit polyclonal antibody. OD_{492}, optical density at 492 nm. (B and C) Sedimentation analyses of the Amut product (B) and of the WT product, used as a control (C). Concentrated supernatants derived from 50-ml cultures were sedimented on continuous sucrose gradients (10% to 60% [wt/vol] in phosphate-buffered saline). The resulting fractions were assessed for specific density and the HEV RNA genome copy number (by real-time reverse transcription-PCR). Note the distinct *y*-axis scales in panels B and C.

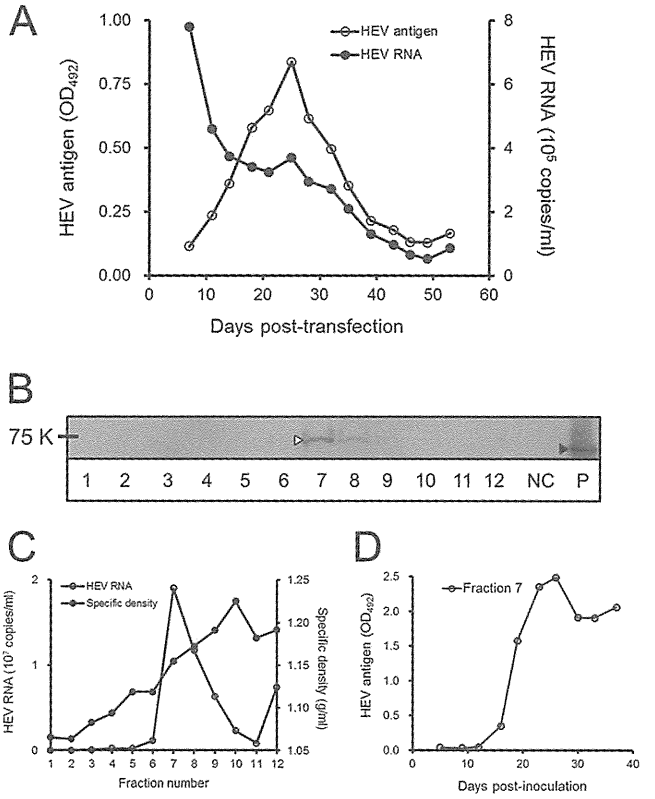

FIG 2 Growth kinetics and character of Amut. (A) Supernatants were collected periodically during 2 months of culturing, and HEV antigen levels were measured by ELISA using an anti-G3-HEV-VLP rabbit polyclonal antibody; the HEV RNA genome copy number was determined by real-time reverse transcription-PCR. OD_{492}, optical density at 492 nm. Supernatants from a pooled total of 3 liters of culture were concentrated and sedimented. (B) Fractions were subjected to Western blotting using an anti-G3-HEV-VLP rabbit polyclonal antibody. NC, negative control (untransfected cells). P, positive control (HEV-L-VLPs). 75 K, 75,000 (molecular weight). Symbols designate the positions of the major band in the Amut supernatant (open arrowhead) and the HEV-L-VLP (filled arrowhead). (C) Fractions were assessed for the HEV RNA genome copy number and specific density. (D) Confirmation of the infectivity of fraction 7 by ELISA.

not detected until 3 weeks posttransfection. The reproducible reversion of Amut provides evidence of the functional essentiality of the C52aa domain for the HEV life cycle.

To permit analysis of the Amut clone in the absence of revertants, culture supernatants collected within the first 10 days were pooled and subjected to partial purification and SDGA. WB detected multiple bands of approximately 55 kDa and smaller, starting in F7; these bands formed a broad range, with peak accumulation detected in F10 (specific density, 1.21 g/ml) (Fig. 3A). In contrast, F8 (specific density, 1.15 g/ml) had the highest copy number of the genome (Fig. 3B). For subsequent analysis, F8 and F10 were designated the minor and major products (Mip and Map, respectively) based on antigen levels. To determine the RNase sensitivities of the products, the fractions were treated with 20 μg/ml of RNase A for 30 min at 37°C. The RNase resistance of the fractions was confirmed by RT-PCR quantification analysis, indicating viral encapsidation. Both products exhibited resistance to RNase treatment (Fig. 3C), indicating the presence of encapsidated RNA. Neither the GAC nor the GUC reversion mutation was detected in these products by RT-PCR sequencing analysis, suggesting that those specific alleles were largely absent from this population.

Further analysis of peak discrepancy between the antigen level and the genome copy number revealed two points. First, the copy

TABLE 2 Time course sequence of the codon mutated to an amber codon for the supernatants of Amut-transfected cells

	Sequence[a] at the following day posttransfection:								
Codon	7	10	14	17	21	24	28	31	35
Amber mutant	UAA	UAA	UAA	UAA	UAA	ND	ND	ND	ND
Revertant									
Intermediate	ND	ND	ND	ND	ND	GAC	GAC	ND	ND
Complete	ND	ND	ND	ND	ND	GUC	GUC	GUC	GUC

[a] Determined for the first codon of the C52aa-encoding region of the ORF2 gene. ND, not detected.

number in the Map fraction was approximately 15 times lower than that in the Mip fraction (Fig. 3B). Second, the constitution (genome/antigen) ratio in the Map fraction was approximately 40-fold lower than that in the Mip fraction by analysis using Image Gauge, version 4.0 (Fujifilm, Tokyo, Japan); the ratio in the Mip fraction was approximately equal to that of WT (Fig. 3D). On the other hand, the RNA content of the Map fraction was extremely reduced, suggesting that these products represented empty parti-

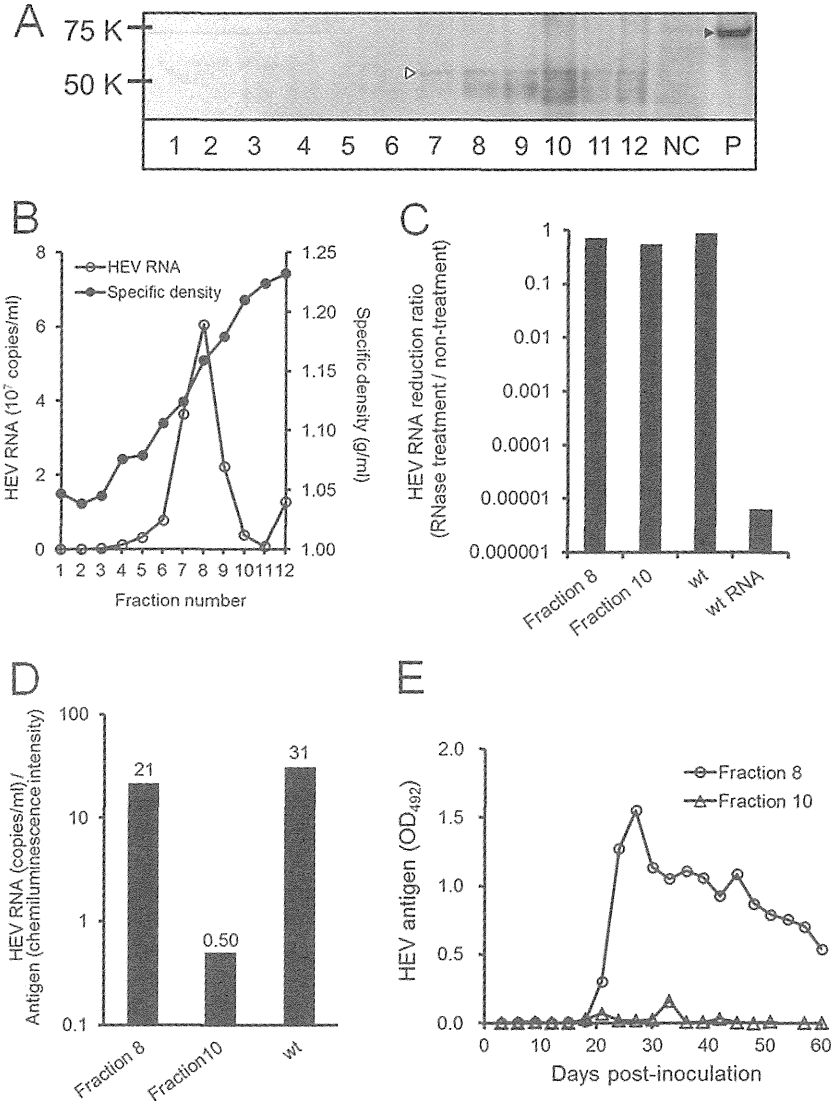

FIG 3 Encapsidation of the Amut genome and its characteristics. (A) Fractions were subjected to Western blotting using an anti-G3-HEV-VLP rabbit polyclonal antibody. NC, negative control (uninfected cells). Symbols indicate the positions of the major bands in the Amut fraction (55 kDa) (open arrowhead) and the WT fraction, used as a positive (P) control (72 kDa) (filled arrowhead). (B) Fractions were assessed for the HEV RNA genome copy number and specific density. (C) RNase resistance was measured as the ratio of the level of HEV RNA in RNase-treated fractions to that in untreated fractions (HEV RNA reduction ratio). WT virions and extracted WT RNA were used as positive and negative controls, respectively. (D) Constitution (genome/antigen) ratios (actual values are shown above the bars) were calculated by dividing the genome quantities from panel B by the chemiluminescence intensities from panel A. (E) To confirm the infectivity of the indicated fractions, cells were inoculated and periodically analyzed by ELISA using an anti-G3-HEV-VLP rabbit polyclonal antibody. OD_{492}, optical density at 492 nm.

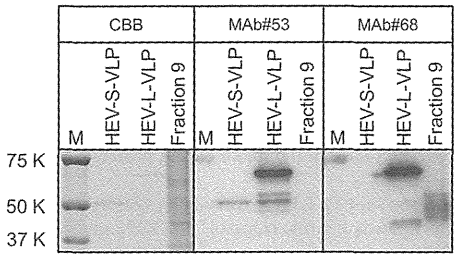

FIG 4 Detection of degraded capsid termini in Amut. HEV small virus-like particles (HEV-S-VLP), HEV large virus-like particles (HEV-L-VLP), and fraction 9 (derived as described for Fig. 3A) were stained with Coomassie brilliant blue (CBB) or were subjected to Western blot analysis using a monoclonal antibody specific to both HEV-S-VLP and HEV-L-VLP (MAb 53) or to HEV-L-VLP alone (MAb 68). Lane M, molecular weight markers.

cles; this inference is consistent with the low productivity of Amut products on all scales. Specifically, we observed that the Map fraction could not infect cells (Fig. 3E), while the Mip fraction was infectious for these cells (Fig. 3E) and yielded reversion mutants (GUC) during long-term observation (data not shown). While the viral reproduction of Amut was impaired, the Mip fraction could sustain low levels of viral production, leading to the emergence of revertants as shown in the large-scale experiment (Fig. 2A).

The observation, via WB (Fig. 3A), of a "smear" of antigen with a maximum size of 55 kDa was unexpected, given that the capsid protein lacking C52aa (predicted size, 6 kDa) was expected to migrate at 66 kDa (that is, 72 kDa less 6 kDa). The observed 11-kDa decrease in size suggested further degradation of the capsid in the absence of the C52aa domain. Mass spectroscopy followed by protein sequencing detected two fragments with amino acid sequences corresponding to early N-terminal capsid sequences. The presence of the capsid N-terminal domain was confirmed by detection with monoclonal antibody (MAb) 68 (Fig. 4), a reagent that exhibits specificity for HEV-L-VLP (specific to the N-terminal 13 to 111 aa) (T. C. Li, unpublished observations). In contrast, the protein was not detected using the HEV-S-VLP- and HEV-L-VLP-specific MAb 53 (Fig. 4), implying the absence of the S-and-L common region. Protein sequencing and reactivity with the HEV-VLP-specific antibodies strongly suggested that the 55-kDa bands correspond to proteolytic products generated by degradation from the C terminus on the viral surface, presumably via loss of the P domain. Further degradation (to lower-molecular-weight species) probably occurred after encapsidation, given that previous studies showed that this region was essential for dimerization and particle formation by the capsid (3, 15, 16).

HEV virions exhibit distinct buoyant densities in feces (1.26 to 1.27 g/ml) and in circulating blood (1.15 to 1.16 g/ml), differences that might be associated with their cellular membrane content (17). The density of the Amut Map fraction was higher than that of the Mip fraction. This result is inconsistent with the notion that the Map is an empty particle (18). The Amut Mip fraction had the specific density of membrane-associated virions, although the ORF3 (egress-related) protein was not detected in these particles, in contrast to WT particles (T. Shiota, unpublished observations) (19). We hypothesize that the correct encapsidation of Amut resulted in an enveloped particle lacking the ORF3 protein (Mip; density, 1.15 g/ml), whereas the incorrect encapsidation of Amut resulted in an nonenveloped and (usually) empty particle (Map; density, 1.21 g/ml), the density of which was intermediate between that of the membrane-associated virion (1.15 to 1.16 g/ml) and the nonenveloped filled virion (1.26 to 1.27 g/ml) (17).

In the present study, we showed that the C52aa domain of the HEV capsid was essential for the HEV life cycle, as confirmed by reproducible reversion at the amber mutation, which would otherwise truncate the C52aa domain. The presence of the C52aa domain promoted the accurate encapsidation of HEV and protected the particle from further C-terminal degradation. To clarify the involvement of the C52aa domain in neutralization, further studies (e.g., using a MAb specific for this region) will be required.

ACKNOWLEDGMENTS

We thank N. Sugiyama for excellent technical support and I. Shiota for helpful discussions and critical reading.

This work was supported in part by grants-in-aid from the Ministry of Health, Labor, and Welfare and the Ministry of Education, Culture, Sports, Science, and Technology, Japan.

REFERENCES

1. Chandra V, Taneja S, Kalia M, Jameel S. 2008. Molecular biology and pathogenesis of hepatitis E virus. J. Biosci. 33:451–464.
2. Tanaka T, Takahashi M, Kusano E, Okamoto H. 2007. Development and evaluation of an efficient cell-culture system for hepatitis E virus. J. Gen. Virol. 88:903–911.
3. Li TC, Takeda N, Miyamura T, Matsuura Y, Wang JC, Engvall H, Hammar L, Xing L, Cheng RH. 2005. Essential elements of the capsid protein for self-assembly into empty virus-like particles of hepatitis E virus. J. Virol. 79:12999–13006.
4. Xing L, Li TC, Mayazaki N, Simon MN, Wall JS, Moore M, Wang CY, Takeda N, Wakita T, Miyamura T, Cheng RH. 2010. Structure of hepatitis E virion-sized particle reveals an RNA-dependent viral assembly pathway. J. Biol. Chem. 285:33175–33183.
5. Li TC, Yamakawa Y, Suzuki K, Tatsumi M, Razak MA, Uchida T, Takeda N, Miyamura T. 1997. Expression and self-assembly of empty virus-like particles of hepatitis E virus. J. Virol. 71:7207–7213.
6. Mori Y, Matsuura Y. 2011. Structure of hepatitis E viral particle. Virus Res. 161:59–64.
7. Xing L, Kato K, Li T, Takeda N, Miyamura T, Hammar L, Cheng RH. 1999. Recombinant hepatitis E capsid protein self-assembles into a dual-domain T=1 particle presenting native virus epitopes. Virology 265:35–45.
8. Guu TS, Liu Z, Ye Q, Mata DA, Li K, Yin C, Zhang J, Tao YJ. 2009. Structure of the hepatitis E virus-like particle suggests mechanisms for virus assembly and receptor binding. Proc. Natl. Acad. Sci. U. S. A. 106:12992–12997.
9. Yamashita T, Mori Y, Miyazaki N, Cheng RH, Yoshimura M, Unno H, Shima R, Moriishi K, Tsukihara T, Li TC, Takeda N, Miyamura T, Matsuura Y. 2009. Biological and immunological characteristics of hepatitis E virus-like particles based on the crystal structure. Proc. Natl. Acad. Sci. U. S. A. 106:12986–12991.
10. Xing L, Wang JC, Li TC, Yasutomi Y, Lara J, Khudyakov Y, Schofield D, Emerson SU, Purcell RH, Takeda N, Miyamura T, Cheng RH. 2011. Spatial configuration of hepatitis E virus antigenic domain. J. Virol. 85:1117–1124.
11. Agrawal S, Gupta D, Panda SK. 2001. The 3′ end of hepatitis E virus (HEV) genome binds specifically to the viral RNA-dependent RNA polymerase (RdRp). Virology 282:87–101.
12. Emerson SU, Zhang M, Meng XJ, Nguyen H, St Claire M, Govindarajan S, Huang YK, Purcell RH. 2001. Recombinant hepatitis E virus genomes infectious for primates: importance of capping and discovery of a *cis*-reactive element. Proc. Natl. Acad. Sci. U. S. A. 98:15270–15275.
13. Graff J, Nguyen H, Kasorndorkbua C, Halbur PG, St Claire M, Purcell RH, Emerson SU. 2005. In vitro and in vivo mutational analysis of the 3′-terminal regions of hepatitis E virus genomes and replicons. J. Virol. 79:1017–1026.
14. Kumar A, Panda SK, Durgapal H, Acharya SK, Rehman S, Kar UK. 2010. Inhibition of hepatitis E virus replication using short hairpin RNA (shRNA). Antiviral Res. 85:541–550.

15. **Li SW, Zhang J, He ZQ, Gu Y, Liu RS, Lin J, Chen YX, Ng MH, Xia NS.** 2005. Mutational analysis of essential interactions involved in the assembly of hepatitis E virus capsid. J. Biol. Chem. **280**:3400–3406.
16. **Graff J, Zhou YH, Torian U, Nguyen H, St Claire M, Yu C, Purcell RH, Emerson SU.** 2008. Mutations within potential glycosylation sites in the capsid protein of hepatitis E virus prevent the formation of infectious virus particles. J. Virol. **82**:1185–1194.
17. **Takahashi M, Tanaka T, Takahashi H, Hoshino Y, Nagashima S, Jirintai, Mizuo H, Yazaki Y, Takagi T, Azuma M, Kusano E, Isoda N, Sugano K, Okamoto H.** 2010. Hepatitis E virus (HEV) strains in serum samples can replicate efficiently in cultured cells despite the coexistence of HEV antibodies: characterization of HEV virions in blood circulation. J. Clin. Microbiol. **48**:1112–1125.
18. **Jacobson MF, Baltimore D.** 1968. Morphogenesis of poliovirus. I. Association of the viral RNA with coat protein. J. Mol. Biol. **33**:369–378.
19. **Tyagi S, Korkaya H, Zafrullah M, Jameel S, Lal SK.** 2002. The phosphorylated form of the ORF3 protein of hepatitis E virus interacts with its non-glycosylated form of the major capsid protein, ORF2. J. Biol. Chem. 277:22759–22767.
20. **Li T-C, Song S, Yang Q, Ishii K, Takeda N, Wakita T.** 2011. A cell culture system for hepatitis E virus. Hepatol. Int. 5:202. doi:10.1007/s12072-010-9241-z.

American Journal of Tropical Medicine & Hygiene

The American Journal of
Tropical Medicine and Hygiene

Molecular detection of Hepatitis E virus in rivers in the Philippines

Journal:	*American Journal of Tropical Medicine & Hygiene*
Manuscript ID:	AJTMH-13-0562.R1
Manuscript Type:	Short Report
Date Submitted by the Author:	n/a
Complete List of Authors:	Li, Tian-cheng; National institute of infectiouse diseases, Department of virology 2 Yang, Tingting; Affiliated Hospital of Qingdao University Medical College, Department of Clinical Laboratory Shiota, Tomoyuki; National Institute of Infectious Diseases, Virology 2 Yoshizaki, Sayaka; National Institute of Infectious Diseases, Virology 2 Hiromu, Yoshida; Department of Virology II, National Institute of Infectious Diseases, Tokyo, Japan, Mariko, Saito; Tohoku University Graduate School of Medicine, Virology Imagawa, Toshifumi; Tohoku University Graduate School of Medicine, Virology Malbas, Fidelino; 5Research Institute for Tropical Medicine, Health Compound Lupisan, Socorro; 5Research Institute for Tropical Medicine, Health Compound Oshitani, Hitoshi; Tohoku University Graduate School of Medicine, Virology Wakita, Takaji; National Institute of Infectious Diseases, Virology 2 Ishii, Koji; National Institute of Infectious Diseases, Virology 2
Key Words:	Emerging Diseases, Hepatitis, Waterborne Infections

Molecular detection of Hepatitis E virus in rivers in the Philippines

Tian-Cheng Li[1], Tingting Yang[1, 2], Tomoyuki Shiota[1], Sayaka Yoshizaki[1], Hiromu Yoshida[1], Mariko Saito[3, 4], Toshifumi Imagawa[3], Fidelino F. Malbas[5], Socorro P. Lupisan[5], Hitoshi Oshitani[3, 4], Takaji Wakita[1], and Koji Ishii[1]*

[1]Department of Virology II, National Institute of Infectious Diseases, Gakuen 4-7-1, Musashi-murayama, Tokyo 208-0011, Japan.

[2]Department of Clinical Laboratory, Affiliated Hospital of Qingdao University Medical College, Jiangsu Road 16, Qingdao 266003,China.

[3]Department of Virology, Tohoku University Graduate School of Medicine, 2-1 Seiryoumachi, Aoba, Sendai, Miyagi 980-8575, Japan.

[4]RITM-Tohoku Collaborating Research Center on Emerging and Re-Emerging Infectious Diseases, Filinvest Corporate City, Alabang, Muntinlupa City 1781, Philippines.

[5]Research Institute for Tropical Medicine, Department of Health Compound, FILINVEST Corporate City, Alabang, Muntinlupa City 1781, the Philippines.

Keywords: Hepatitis E Virus, Genotype 3, Philippines, 4, wastewater.

Running title: HEV infection in the Philippines.

***Correspondence author:** Koji Ishii. Department of Virology II, National Institute of Infectious Diseases, 4-7-1 Gakuen, Musashi-murayama, Tokyo 208-0011, Japan

Phone: +81-42-561-0771, Fax: +81-42-565-4729, E-mail: litc@nih.go.jp

Abstract

To understand the HEV-pollution status in the environment in the Philippines, a total of 12 water samples were collected from rivers in Manila City for detection of HEV RNA. Three out of 12 samples were positive for HEV RNA indicating that HEV is circulating in the Philippines. Phylogenetic analysis classified all of the HEV sequences into genotype 3.

Hepatitis E virus (HEV) is a positive-sense single-stranded RNA virus that belongs to the genus *Hepevirus* in the family *Hepeviridae* [1,2,3]. HEV is the causative agent of acute or fulminant hepatitis E, primarily transmitted by the fecal-oral route[4]. The relatively high mortality rate in HEV-infected pregnant women, up to 28%, is unique among hepatitis viruses [1,5]. Hepatitis E is a zoonotic disease, with swine, wild boars and wild deer serving as the reservoir for human infections [6,7,8]. Four genotypes of HEV (G1-G4) have been detected in humans and G3 and G4 HEV are responsible for sporadic and autochthonous infections in both humans and other animal species worldwide [9,10,11,12].

HEV is a public health concern in many Asia and Africa countries where sanitation conditions are insufficient [13,14]. Large waterborne outbreaks with high attack rates among young adults have been described in regions characterized by poor sanitary conditions in countries such China, Indian, Somalia, and Uganda[15]. However, there have been no reports of HEV infection in the Philippines. Neither information about hepatitis E patients, nor HEV infection in animals has been reported, and no sequence data has been deposited from this country. There is also no report of the HEV-pollution status of the environmental sewage water. With the hypothesis that environmental water samples may reflect the prevalence of HEV circulation, we examined river water samples to investigate HEV in the environment in one of the most densely populated cities in the world Manila City, a metropolitan area in the Philippines with over 10 million residents.

A total of 12 water samples were collected from rivers that run through Manila City. Six sampling sites were selected (Fig. 1). Sampling sites 1 to 3 were in the Pasig River, sites 4 and 5 were in the Paranaque River, and site 6 was in the Las Pinas River. These rivers receive the wastewater from the residents nearby. Water samples were drawn at all locations during both the dry season (2012.12.23) and the wet season (2013.07.23), and were named

D1 to D6 and W1 to W6, respectively. The water samples were kept at 4°C during transport.

The concentration and purification of these water samples was carried out as described previously[16]. Briefly, 500 mL of water was collected from each sampling site, and centrifuged at 3,000 rpm for 30 min at 4°C. Then 2.5 mM $MgCl_2$ was added to the supernatant to a final concentration of 0.05 mM. The pH value was adjusted to 3.5. The solution was filtered through a 0.45-μm mixed cellulose ester membrane filter (Merck Millipore Japan) by a positive-pressure pump. Absorbents on the filter were then eluted with 10 mL of 3% beef extract solution by ultrasonication, three times. The solution was centrifuged at 12,000 rpm for 30 min, and the supernatant was stored at −80°C until RNA extraction.

The RNA was extracted using the MagNA Pure LC Total Nucleic Acid isolation kit (Roche Applied Science, Mannheim, Germany) according to the manufacturer's recommendations. Reverse transcription (RT) was performed with a high-capacity cDNA reverse transcription kit (ABI Applied Biosystems) at 25 °C for 10 min, 37 °C for 120 min followed by 85 °C for 5 min in a 20-μl reaction mixture containing 1 μl reverse transcriptase, 2 μl of the random primer, 1 μl RNase inhibitor, 2 μl RT buffer, 0.8 μl 10-mM deoxynucleoside triphosphates, 8 μl RNA and 5.2 μl distilled water. A nested reverse transcription polymerase Chain Reaction (RT-PCR) analysis was performed to amplify a portion of the ORF2 genome, based on the method described previously[17].

By RT-PCR, three samples (W4, W5 and W6) out of the 12 water samples were positive for HEV RNA. Excluding the primer sequences, the length of the nested RT-PCR products was 338 nucleotides corresponding to nt 5959-6296 in the ORF2 of the Myanmar strain (D10330). PCR products were purified using the QIAquick PCR purification kit (Qiagen) and cloned into TA cloning vector pCR2.1 (Invitrogen). Each of 20 clones was sequenced. The clones with the same nucleotide sequence were

86 counted as one strain. Finally, 21 HEV strains were obtained (GenBank accession nos.
87 KF546257-KF546277), of which five strains were isolated from W4, 10 strains from
88 W5, and six strains from W6. Phylogenetic analysis indicated that all 21 strains were
89 G3 HEV. With the exception of strain W5-13, the other 20 strains' sequences belonged
90 to sub-genotype 3a[18], separated into four clusters (Cluster1 to 4) with nucleotides
91 sequence identities of 89.6%-99.7% (Fig. 2). In cluster 1, the sequences of three strains
92 isolated from W6 were close to that of HEV strain EF530663 (isolated from a patient in
93 Hungary) with nucleotide sequence identities of 92.3% to 92.6%. The nucleotide
94 sequences of all nine of the strains in cluster 2 detected from W5 were close to that of a
95 Japan swine HEV strain (AB094215) with identities of 91.1%-92.6%. Cluster 3
96 contained six strains three from W4 and three from W6. Their sequences were close to
97 that of AB671098, isolated from a Japanese donor, with nucleotide sequence identities
98 of 93.5%-94.4%. Cluster 4 comprised two strains from W4, with sequences close to
99 Japan strain AB 807429 (identities of 91.7%-92.0%). The strain W5-13 dose not belong
100 to any known sub-genotype and shares identities of 84.0%-84.3%, 90.2%-91.7%,
101 85.5%-88.2% and 83.7%-84.0%, with the Philippines HEV strains in clusters 1 to 4,
102 respectively. The strain W5-13 thus constitutes a new sub-genotype of G3 HEV.
103 A BLAST analysis showed that the nucleotide sequence identities between these
104 HEV strains detected in the Philippines and other HEV strains that have been published
105 in GenBank were lower than 94.4%, indicating that area-specific HEV strains are
106 circulating in the Philippines. All 21 of the HEV strains we detected in the river water
107 were collected during the wet season, suggesting that the wet season presents a higher
108 risk of individuals in the area contracting HEV infections.
109 The results of this study beg the question, what is the source of HEV detected in the
110 Manila City rivers? Because no epidemiological information about HEV in the
111 Philippines is currently available, for human patients, animal outbreaks, or genetic
112 sequences, it is difficult to speculate about the sources of HEV. However, since the

HEV is primarily transmitted by the fecal-oral route, HEV might be present in rivers containing human or animal stool. In this study, all of the HEV strains were detected from sampling sits 4-6, located in the Paranaque River and the Las Pinas River. None of the water samples from the Pasig River (sampling sits 1-3) were found to be HEV RNA positive. The Paranaque River and the Las Pinas River are considerably smaller than the Pasig River, and flow through a residential area having high population density. The degree of wastewater pollution is higher for sampling sits 4-6 than for sampling sits 1-3. All of the HEV detected in the river water samples belonged to G3. Genotype 3 HEV can be isolated not only from infected humans but is known to be zoonotic and has also been isolated from domestic swine, and wild boars, wild deer, mongoose, and rabbits [6, 7, 9, 11, 19, 20]. The rivers were probably contaminated with HEV by human or animal excrement, or both.

In conclusion, we have detectedand here report HEV in the Philippines for the first time, and showed that G3 HEV in particular is circulating in the rivers of Manila City. In order to fully elucidate and address the HEV infection situation in the Philippines, it will be necessary to collect and analyze hepatitis patients' information and investigate the prevalence of HEV infection in swine and wild animals in these areas.

Acknowledgments

We would like to thank Dr. Hiroyuki Katayama (University of Tokyo) for helpful discussions. This work was supported in part by grants from the Ministry of Health, Labour and Welfare of Japan, and the Japan Initiative for Global Research Network on Infectious Diseases (J-GRID) from the Ministries of Education, Culture, Sports, Science and Technology of Japan.

Authors' current addresses

Tian-Cheng Li, Department of Virology II, National Institute of Infectious Diseases, Gakuen 4-7-1, Musashi-murayama, Tokyo 208-0011, Japan. E-mail: litc@nih.go.jp; Tingting Yang, [2]Department of Clinical Laboratory, Affiliated Hospital of Qingdao University Medical College, Jiangsu Road 16, Qingdao 266003,China. E-mail: ttyang629@126.com.Tomoyuki Shiota, Department of Virology II, National Institute of Infectious Diseases, E-mail: t-shiota@nih.go.jp. Sayaka Yoshizaki, Department of Virology II, National Institute of Infectious Diseases, E-mail: yoshizak@nih.go.jp. Hiromu Yoshida[1], Mariko Saito, Department of Virology, Tohoku University Graduate School of Medicine, 2-1 Seiryoumachi, Aoba, Sendai, Miyagi 980-8575, Japan. E-mail: saitom@med.tohoku.ac.jp. Toshifumi Imagawa, Department of Virology, Tohoku University Graduate School of Medicine, E-mail: imagawat@med.tohoku.ac.jp. Fidelino F. Malbas, RITM-Tohoku Collaborating Research Center on Emerging and Re-Emerging Infectious Diseases, Filinvest Corporate City, Alabang, Muntinlupa City 1781, Philippines. E-mail: fidelmalbas@yahoo.com. Socorro P. Lupisan, RITM-Tohoku Collaborating Research Center on Emerging and Re-Emerging Infectious Diseases, E-mail: socorrolupisan@yahoo.com. Hitoshi Oshitani, Department of Virology, Tohoku University Graduate School of Medicine, E-mail: oshitanih@med.tohoku.ac.jp . Takaji Wakita, Department of Virology II, National Institute of Infectious Diseases, E-mail: wakita@nih.go.jp. Koji Ishii, Department of Virology II, National Institute of Infectious Diseases, E-mail: kishii@nih.go.jp.